Journal of the Physical Society of Japan **87**, 033704 (2018) **Letters**
https://doi.org/10.7566/JPSJ.87.033704

Anisotropic Magnetic Fluctuations in Ferromagnetic Superconductor UGe_2: ^{73}Ge-NQR Study at Ambient Pressure

Yuichiro Noma[1], Hisashi Kotegawa[1], Tetsuro Kubo[1], Hideki Tou[1], Hisatomo Harima[1], Yoshinori Haga[2], Etsuji Yamamoto[2], Yoshichika Ōnuki[3], Kohei M. Itoh[4], Eugene E. Haller[5], Ai Nakamura[6], Yoshiya Homma[6], Fuminori Honda[6], and Dai Aoki[6]

[1]*Department of Physics, Kobe University, Kobe 657-8501, Japan*
[2]*Advanced Science Research Center, Japan Atomic Energy Agency, Tokai, Ibaraki 319-1195, Japan*
[3]*Faculty of Science, University of the Ryukyus, Nishihara, Okinawa 903-0213, Japan*
[4]*School of Fundamental Science and Technology, Keio University, Yokohama 223-8522, Japan*
[5]*Lawrence Berkeley Laboratory, University of California, Berkeley, CA 94720, U.S.A.*
[6]*Institute for Materials Research, Tohoku University, Oarai, Ibaraki 311-1313, Japan*

(Received December 28, 2017; accepted January 15, 2018; published online February 16, 2018)

We report a ^{73}Ge nuclear quadrupole resonance reinvestigation of the ferromagnetic (FM) superconductor UGe_2 at ambient pressure. Careful measurement and analysis of the paramagnetic (PM) spectrum taking into account the calculated electric field gradient (EFG) resulted in modification of the previously reported site assignments for three inequivalent Ge sites. The crossover anomaly at T_x in the FM state is not clearly seen in the temperature dependence of the static internal field at the Ge site, whereas it appears in the nuclear spin–lattice relaxation rate, $1/T_1$. A remarkable site dependence of $1/T_1$ is observed among the inequivalent Ge sites, where the directions of the principal axes of the EFG are different. This result reveals that the magnetic fluctuation of UGe_2 is highly anisotropic, which is consistent with the presence of Ising magnetic fluctuations in the PM state.

The coexistence of ferromagnetic (FM) and superconducting (SC) states is a fascinating phenomenon but still rare. It has been reported only in a few U-based compounds such as UGe_2, URhGe, UCoGe, and UIr.[1–4] This indicates that the sufficient condition for realization of superconductivity in the FM state is very strict. All four systems exhibit strong uniaxial magnetic anisotropy, which is most likely important for FM superconductors. Superconductivity generally appears near the magnetic phase boundary, but the detailed situation depends strongly on the material. UCoGe shows a maximum of the SC transition temperature, T_{sc}, near the pressure-induced FM–paramagnetic (PM) transition,[5] whereas URhGe does not show any quantum magnetic phase transition under pressure.[6] On the other hand, the magnetic field along the *b*-axis, which is a hard axis, induces reentrant superconductivity in URhGe and a similar enhancement of T_{sc} in UCoGe.[7–9] These SC states are accompanied by field-induced suppression of the FM state. Near a continuous quantum phase transition, quantum fluctuations are expected, and they may be a driving force of superconductivity. In fact, ^{59}Co nuclear magnetic resonance (NMR) of UCoGe has revealed a strong connection between the Ising-type magnetic fluctuation and superconductivity.[10,11] For the field-enhanced superconductivity, NMR measurements have also shown that magnetic fluctuations develop under a magnetic field along the *b*-axis in UCoGe and URhGe.[12–14] In URhGe, the spin reorientation of the U moment from the *c*-axis to the *b*-axis under a field along the *b*-axis is of the discontinuous first order,[8,13–17] but the transition is most likely of the weak first-order type, and the development of magnetic fluctuation is clearly observed there.

On the other hand, the first known FM superconductor, UGe_2, is still far from a solution. This material possesses two types of FM phases with ordered moments of different sizes: FM1 and FM2. Superconductivity is observed only in the FM state with the relatively large U moment of $0.9\,\mu_B$, and the maximum T_{sc} is achieved near P_x, which is a boundary between the FM1 and FM2 phases at 0 K. The boundary is considered to be of first order at 0 K, and changes to crossover as the temperature is elevated through a critical point, which is most likely located at $P = 1.15$ GPa and $T = 7$ K.[18] The fluctuation induced at the critical point may be a driving force of the superconductivity; however, it is unclear whether such fluctuations can survive at low temperatures (far below 7 K). In previous nuclear quadrupole resonance (NQR) measurements of UGe_2,[19–21] the temperature-divided nuclear spin–lattice relaxation rate $1/T_1T$ showed a significant change between the FM1 and FM2 phases, but the change at low temperature was step-like against pressure, and it did not show a clear anomaly such as divergent behavior. The pressure dependence of the electronic specific heat coefficient and the *A* coefficient of resistivity also shows step-like behavior at P_x,[22–24] which is in sharp contrast to the case of the weak first-order spin reorientation in URhGe.[25,26] Even at a temperature where the critical point is expected, clear divergence has not been detected by measurements of $1/T_1T$; only a gradual evolution of $1/T_1T$ appears near the T_x line.[19] Therefore, there is no direct indication of a factor that drives the superconductivity of UGe_2. To solve this issue, we restarted ^{73}Ge-NQR/NMR measurements. In this paper, before describing a high-pressure study, we present the results of a careful reinvestigation of NQR of UGe_2 at ambient pressure.

Samples for the NQR measurements were made using enriched ^{73}Ge. We used mainly powdered polycrystalline samples for the measurements, and powdered single crystals were also used to confirm the spectrum. Both types of samples were annealed at a high temperature of ∼900 °C to reduce deformation after powdering. All the NQR measurements were performed by the spin-echo method at zero magnetic field. The nuclear spin and gyromagnetic ratio of ^{73}Ge are $I = 9/2$ and $\gamma_n/2\pi = 1.4852$ MHz/T, respectively.

Figure 1 shows the crystal structure of UGe_2, which is orthorhombic in the space group *Cmmm* (No. 65). Three

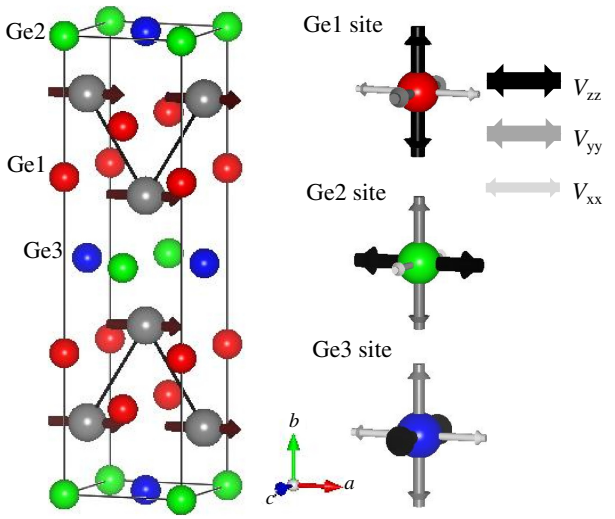

Fig. 1. (Color online) Crystal structure of UGe_2 and the direction of the EFG at each Ge site. The equivalent U atoms form a zigzag chain along the a-axis, and the ordered moments are directed along the a-axis in the FM state. The crystal possesses three inequivalent Ge sites, whose principal axes of the EFG lie along the crystal axes, but the directions are different from each other.

Table I. Directions of the principal axes and the EFG parameters derived from the band calculation for three Ge sites. The experimental values are also shown.

Site	Wyckoff	Local symmetry	LDA Calculation					Experiment	
			V_{zz}	V_{yy}	V_{xx}	ν_Q (MHz)	η	ν_Q (MHz)	η
Ge1	4*i*	*m*2*m*	*b*	*c*	*a*	2.36	0.953	2.29	0.967
Ge2	2*a*	*mmm*	*a*	*b*	*c*	3.48	0.678	3.11	0.818
Ge3	2*c*	*mmm*	*c*	*b*	*a*	3.63	0.719	3.29	0.915

inequivalent Ge sites labeled Ge1, Ge2, and Ge3 are included in a unit cell; their Wyckoff letters and local symmetries are shown in Table I. The electric field gradient (EFG) at each site is a key factor for understanding the NQR data, especially the nuclear spin–lattice relaxation rate, $1/T_1$. Its magnitude and direction are calculated through a full-potential linear augmented plane wave calculation within the local density approximation (LDA), as shown in Fig. 1 and Table I. The black bar indicates the direction of V_{zz}, which is the maximum principal axis of the EFG, and dark gray and light gray represent V_{yy} and V_{xx}, which are the principal axes with the second-largest and the smallest EFG: $|V_{zz}| \geq |V_{yy}| \geq |V_{xx}|$. From the local symmetry at the Ge sites, each principal axis is restricted along the directions equal to the crystal axes for all three Ge sites, but they are not in axial symmetry; that is, the asymmetry parameter $\eta = (|V_{yy}| - |V_{xx}|)/|V_{zz}|$ $(0 \leq \eta \leq 1)$ is nonzero. The calculated values of the quadrupole frequency ν_Q and η are also listed in Table I. The η values are relatively large for all the Ge sites.

Figures 2(a) and 2(b) show the NQR spectra in the PM state ($T = 70$ K) and in the FM state ($T = 5$ K). In the previous NQR measurements,[19–21] the spectrum in the PM state was obtained only under pressure; therefore, these are the first NQR data for the PM state at ambient pressure. The previous measurements were limited to frequencies no higher than 11 MHz, but we found two new signals at approximately 12 MHz. As a result, the site assignments were modified from

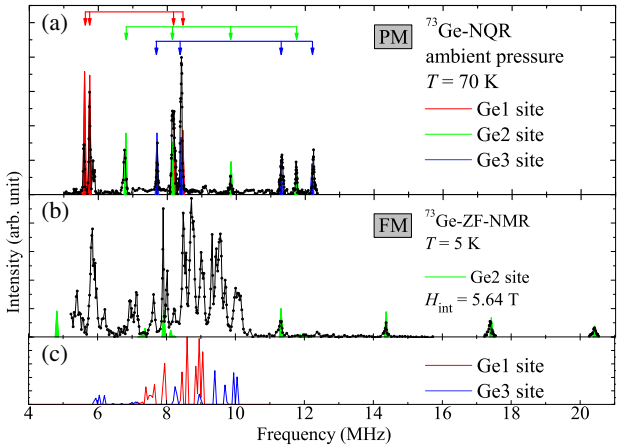

Fig. 2. (Color online) (a) ^{73}Ge-NQR spectrum at $T = 70$ K in the PM state. The colored lines indicate the simulations for each Ge site. (b) ^{73}Ge-ZF-NMR spectrum at $T = 5$ K in the FM state. A complicated spectrum is obtained because of the presence of H_{int}, but the spectrum for the Ge2 site is reproduced well using the following parameters for Ge2: $\nu_Q = 3.08$ MHz, $\eta = 0.818$, $\theta = 0°$, $\phi = 0°$, and $H_{int} = 5.64$ T, where θ and ϕ are the angles between the EFG principal axes and H_{int}. At the Ge2 site, the angles of $\theta = 0°$ and $\theta = 0°$ correspond to $H_{int} \parallel V_{zz} \parallel a$. (c) Tentative simulation of the Ge1 and Ge3 sites in the FM state. The parameters are as follows: Ge1: $\nu_Q = 2.25$ MHz, $\eta = 0.95$, $\theta = 80°$, $\phi = 80°$, and $H_{int} = 5.25$ T, Ge3: $\nu_Q = 3.35$ MHz, $\eta = 0.88$, $\theta = 82°$, $\phi = 84°$, and $H_{int} = 5.08$ T. At both sites, $\theta = 90°$ and $\phi = 90°$ correspond to $H_{int} \parallel V_{xx} \parallel a$.

the previous ones.[19–21] The colored curves indicate simulations of each Ge site to reproduce the experimental spectrum. By taking into account the calculated values, we determined ν_Q and η values at each site, as shown in Table I. They reproduce the experimental spectrum well and are in moderately good agreement with the calculation. Note that the enhancement of H_1 appears at the sites denoted as Ge1 and Ge3 near T_{Curie}, but it is not significant at the site denoted as Ge2. This is because the low-energy magnetic fluctuations near T_{Curie} can enhance the rf field along the easy a-axis, which is effective for the Ge1 and Ge3 sites but ineffective for the Ge2 site, whose V_{zz} is along the a-axis, and the resonance at the Ge2 site requires mainly an alternating field normal to the a-axis.

In the FM state, the spectrum is dramatically different because of the appearance of the internal field, H_{int}. More than nine resonance lines are expected for one Ge site with $I = 9/2$ and large η. Most of the resonances appear between 8 and 10 MHz and have a complicated appearance, whereas four peaks with almost equal intervals are seen above 11 MHz, which are the satellite lines induced by zero-field (ZF) NMR. As shown by the green curve, the well-separated satellite lines are reproduced adequately by using the EFG parameters, which are almost the same as those of the Ge2 site in the PM state. In this simulation, $H_{int} = 5.64$ T is simply directed to the a-axis, suggesting that the hyperfine coupling is dominated by an isotropic component. An observation of similar well-separated satellite lines for the Ge2 site in the NMR spectrum, where an external magnetic field is applied along the a-axis of an oriented sample, also supports the suggestion that H_{int} lies almost along the a-axis.[27] The NMR spectrum of the oriented sample also suggests that the magnetic field along the a-axis does not separate the resonance lines well for the Ge1 and Ge3 sites

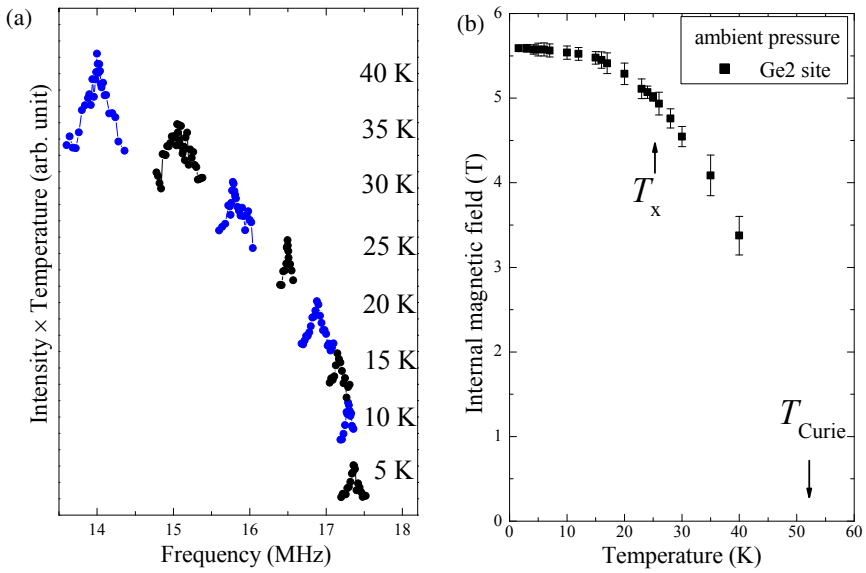

Fig. 3. (Color online) (a) The $-5/2 \Leftrightarrow -7/2$ transition for the Ge2 site measured at several temperatures. The peak position shifts with the magnitude of the internal field, H_{int}, at the Ge2 site. (b) Temperature dependence of the estimated H_{int} at the Ge2 site. A clear anomaly at T_x is not seen within the experimental resolution.

owing to the direction of the EFG tensor.[27] This indicates that the complicated ZF-NMR spectrum below ~10 MHz originates from the Ge1 and Ge3 sites, and the internal field lies almost along the *a*-axis for both sites. The tentative simulation result is displayed in Fig. 2(c). Although it was difficult to reproduce the Ge1 and Ge3 sites adequately by a simulation, the spectrum suggests that H_{int} lies almost along the *a*-axis for the Ge1 and Ge3 sites as well as the Ge2 site; that is, isotropic hyperfine coupling is dominant at all the Ge sites.

Figure 3(a) shows the temperature dependence of the satellite line at the Ge2 site in the FM state, which corresponds to the $-5/2 \Leftrightarrow -7/2$ transition. The peak position shifts to lower frequency with increasing temperature because of a reduction in H_{int}. The H_{int} value at each temperature is estimated from simulations, and the temperature dependence of H_{int} is shown in Fig. 3(b). H_{int} decreases gradually toward T_{Curie}, as in the magnetization measurement.[1,28] A crossover anomaly at $T_x \sim 25$ K has been detected in some measurements even at ambient pressure,[29–31] but no clear anomaly was observed in H_{int} or the magnetization and ordered moment estimated from the neutron scattering.[1,23,28]

To unravel the anisotropy of the magnetic fluctuations in the PM state of UGe_2, the nuclear spin–lattice relaxation rate $1/T_1$ was measured at the Ge2 site ($f = 11.7$ MHz) and at the Ge3 site ($f = 12.2$ MHz), where both signals arise mainly from the $\pm 7/2 \Leftrightarrow \pm 9/2$ transition. In the FM state, T_1 was measured at the satellite line of the Ge2 site (17.2 MHz at 5 K), which is the $-5/2 \Leftrightarrow -7/2$ transition. The temperature dependence is shown in Fig. 4. In the PM state, $1/T_1$ behaves very differently at the Ge2 and Ge3 sites; $1/T_1$ at the Ge3 site increases dramatically toward T_{Curie}, whereas $1/T_1$ at the Ge2 site does not show such strong divergence. Further, $1/T_1$ at the Ge3 site is well fitted by $1/T_1 \propto T/(T - T_{Curie})$, which is anticipated for three-dimensional itinerant ferromagnets on the basis of self-consistent renormalization (SCR) theory.[32]

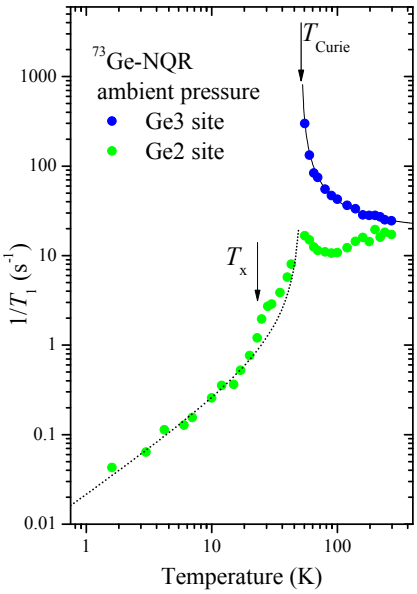

Fig. 4. (Color online) Temperature dependence of $1/T_1$ for the Ge2 and Ge3 sites. The solid line shows $1/T_1 \propto T/(T - T_{Curie})$ at $T > T_{Curie}$, and the dotted line shows $1/T_1 \propto T/(T_{Curie} - T)$ at $T < T_{Curie}$. The two fitted lines show the expected result for three-dimensional itinerant ferromagnets. The contrasting behavior at the Ge2 and Ge3 sites toward T_{Curie} indicates anisotropic magnetic fluctuations developing along the *a*-axis.

However, this is not valid for the Ge2 site owing to a difference in the directions of the EFG tensors between the two sites. In a simple NMR/NQR case with axial symmetry, the nuclear spin is relaxed through magnetic fluctuations perpendicular to the nuclear quantization axis, as follows.

$$\frac{1}{T_1} = \frac{\gamma_n^2}{2} \int_{-\infty}^{\infty} \langle \delta H^-(t) \delta H^+(0) \rangle \exp(-i\omega_n t)\, dt, \qquad (1)$$

where $\langle \delta H^-(t) \delta H^+(0) \rangle$ is a time-correlation function for magnetic fluctuations perpendicular to the nuclear quantiza-

tion axis, and γ_n and ω_n are the gyromagnetic ratio and resonance frequency, respectively. In NQR for $\eta = 0$, the nuclear quantization axis is the direction of V_{zz}. Nuclear spin relaxation is induced by the magnetic fluctuation along both the V_{yy} and V_{xx} directions. As η increases from zero, on the other hand, $|V_{yy}|$ increases toward $|V_{zz}|$, and they become equivalent when $\eta = 1$. This means that the increase in η reduces the contribution of the magnetic fluctuation along V_{yy} to the T_1 process. Chepin et al. have shown the analytical solution of the η dependence of $1/T_1$ for $I = 3/2$.[33] The contributions to the transition probability are related as $S_z : S_y : S_x = 0 : 3 : 3$ for $\eta = 0$, where S_i represents the magnetic fluctuations along the V_{ii} direction, whereas the contributions change to $S_z : S_y : S_x = 1 : 1 : 4$ for $\eta = 1$. For $I = 9/2$, a similar evaluation cannot be easily done because the relaxation curve changes to a multi-exponential function, but we confirmed that this tendency is independent of I. In UGe_2, η at the Ge2 and Ge3 sites is close to 1; therefore, the T_1 values at both sites are dominated by magnetic fluctuations along V_{xx}. From the directions of V_{xx} listed in Table I, the main contribution to $1/T_1$ is the magnetic fluctuations along the a-axis at the Ge3 site, whereas that to $1/T_1$ is along the c-axis at the Ge2 site. Considering that isotropic hyperfine coupling is dominant at all the Ge sites, this contrasting behavior of $1/T_1$ clearly suggests that the magnetic fluctuation of UGe_2 is highly anisotropic, and the fluctuation along the a-axis is much larger than that along the c-axis. The result is consistent with the fact that the magnetic fluctuations have Ising anisotropy in the PM state.

In the FM state, $1/T_1$ decreases toward low temperatures, showing a small shoulder at around $T_x \sim 25$ K. This is clearly seen if we draw the curve of $1/T_1 \propto T/(T_{\mathrm{Curie}} - T)$ expected from SCR theory below T_{Curie}.[32] The crossover anomaly between the FM1 and FM2 phases is seen in $1/T_1$ even at ambient pressure, unlike the static H_{int}. The evolution of the electronic state may appear the dynamical part remarkably in the crossover regime. Regarding the anisotropy of the magnetic fluctuations in the FM state, an important point is that the large internal field tilts the nuclear quantization axis greatly toward the a-axis at all the Ge sites. At the Ge2 site, for example, $H_{\mathrm{int}} = 5.64$ T directed to the a-axis is larger than $\nu_Q/\gamma_n = 3.11/1.4852 \simeq 2.1$ T, indicating that the Zeeman interaction is predominant over the quadrupole interaction. Therefore, $1/T_1$ in the FM state is expected to reflect mainly the magnetic fluctuations along the bc plane. This is not the FM longitudinal fluctuation being considered as the key factor for FM superconductors but the transverse fluctuation. In the previous studies under pressure,[19–21] the $1/T_1$ value measured in the FM state was most likely dominated by the transverse fluctuation. To clarify the longitudinal fluctuations in the FM state, especially near the critical point, measurement of the spin-echo decay rate $1/T_2$ would be a key point, as in URhGe.[13,14]

In summary, we performed ^{73}Ge-NQR measurements of UGe_2. The three Ge sites were successfully assigned while maintaining consistency with the LDA calculation. The contrasting site dependence of $1/T_1$ enables us to reveal the anisotropy of the magnetic fluctuations in the PM state of UGe_2, which suggests the presence of strong longitudinal fluctuations along the a-axis. In the FM state, on the other hand, the large internal field compared with the nuclear quadrupole frequency tilts the quantization axis greatly toward the a-axis. As a result, $1/T_1$ in the FM state is expected to be dominated by the transverse fluctuations. This may explain why a distinct anomaly was absent near the critical point in the previous results for $1/T_1T$. As the next step, a complementary study using $1/T_1$ and $1/T_2$ is important to clarify the anisotropy of the magnetic fluctuations near P_x and to reveal the relationship between the magnetic fluctuations and superconductivity in UGe_2.

Acknowledgements This work was supported in part by Grants-in-Aid for Scientific Research (Nos. 15H03689, 15H05745, 15H05885, and 26400359) from the Ministry of Education, Culture, Sports, Science and Technology (MEXT) of Japan.

1) S. S. Saxena, P. Agarwal, K. Ahilan, F. M. Grosche, R. K. W. Haselwimmer, M. J. Steiner, E. Pugh, I. R. Walker, S. R. Julian, P. Monthoux, G. G. Lonzarich, A. Huxley, I. Sheikin, D. Braithwaite, and J. Flouquet, Nature (London) **406**, 587 (2000).
2) D. Aoki, A. Huxley, E. Ressouche, D. Braithwaite, J. Flouquet, J.-P. Brison, E. Lhotel, and C. Paulsen, Nature (London) **413**, 613 (2001).
3) N. T. Huy, A. Gasparini, D. E. de Nijs, Y. Huang, J. C. P. Klaasse, T. Gortenmulder, A. de Visser, A. Hamann, T. Görlach, and H. Löhneysen, Phys. Rev. Lett. **99**, 067006 (2007).
4) T. Akazawa, H. Hidaka, T. Fujiwara, T. C. Kobayashi, E. Yamamoto, Y. Haga, R. Settai, and Y. Ōnuki, J. Phys.: Condens. Matter **16**, L29 (2004).
5) E. Hassinger, D. Aoki, G. Knebel, and J. Flouquet, J. Phys. Soc. Jpn. **77**, 073703 (2008).
6) F. Hardy, A. Huxley, J. Flouquet, B. Salce, G. Knebel, D. Braithwaite, D. Aoki, M. Uhlarz, and C. Pfleiderer, Physica B **359–361**, 1111 (2005).
7) F. Lévy, I. Sheikin, B. Grenier, and A. D. Huxley, Science **309**, 1343 (2005).
8) F. Lévy, I. Sheikin, B. Grenier, C. Marcenat, and A. Huxley, J. Phys.: Condens. Matter **21**, 164211 (2009).
9) D. Aoki, T. D. Matsuda, V. Taufour, E. Hassinger, G. Knebel, and J. Flouquet, J. Phys. Soc. Jpn. **78**, 113709 (2009).
10) Y. Ihara, T. Hattori, K. Ishida, Y. Nakai, E. Osaki, K. Deguchi, N. K. Sato, and I. Satoh, Phys. Rev. Lett. **105**, 206403 (2010).
11) T. Hattori, Y. Ihara, Y. Nakai, K. Ishida, Y. Tada, S. Fujimoto, N. Kawakami, E. Osaki, K. Deguchi, N. K. Sato, and I. Satoh, Phys. Rev. Lett. **108**, 066403 (2012).
12) T. Hattori, K. Karube, K. Ishida, K. Deguchi, N. K. Sato, and T. Yamamura, J. Phys. Soc. Jpn. **83**, 073708 (2014).
13) H. Kotegawa, K. Fukumoto, T. Toyama, H. Tou, H. Harima, A. Harada, Y. Kitaoka, Y. Haga, E. Yamamoto, Y. Ōnuki, K. M. Itoh, and E. E. Haller, J. Phys. Soc. Jpn. **84**, 054710 (2015).
14) Y. Tokunaga, D. Aoki, H. Mayaffre, S. Krämer, M.-H. Julien, C. Berthier, M. Horvatić, H. Sakai, S. Kambe, and S. Araki, Phys. Rev. Lett. **114**, 216401 (2015).
15) D. Aoki, G. Knebel, and J. Flouquet, J. Phys. Soc. Jpn. **83**, 094719 (2014).
16) A. Gourgout, A. Pourret, G. Knebel, D. Aoki, G. Seyfarth, and J. Flouquet, Phys. Rev. Lett. **117**, 046401 (2016).
17) S. Nakamura, T. Sakakibara, Y. Shimizu, S. Kittaka, Y. Kono, Y. Haga, J. Pospíšil, and E. Yamamoto, Phys. Rev. B **96**, 094411 (2017).
18) V. Taufour, A. Villaume, D. Aoki, G. Knebel, and J. Flouquet, J. Phys.: Conf. Ser. **273**, 012017 (2011).
19) H. Kotegawa, A. Harada, S. Kawasaki, Y. Kitaoka, Y. Haga, E. Yamamoto, Y. Ōnuki, K. M. Itoh, E. E. Haller, and H. Harima, J. Phys. Soc. Jpn. **74**, 705 (2005).
20) A. Harada, S. Kawasaki, H. Kotegawa, Y. Kitaoka, Y. Haga, E. Yamamoto, Y. Ōnuki, K. M. Itoh, E. E. Haller, and H. Harima, J. Phys. Soc. Jpn. **74**, 2675 (2005).
21) A. Harada, S. Kawasaki, H. Mukuda, Y. Kitaoka, Y. Haga, E. Yamamoto, Y. Ōnuki, K. M. Itoh, E. E. Haller, and H. Harima, Phys. Rev. B **75**, 140502(R) (2007).
22) N. Tateiwa, T. C. Kobayashi, K. Hanazono, K. Amaya, Y. Haga, R. Settai, and Y. Ōnuki, J. Phys.: Condens. Matter **13**, L17 (2001).

23) A. Huxley, I. Sheikin, E. Ressouche, N. Kernavanois, D. Braithwaite, R. Calemczuk, and J. Flouquet, Phys. Rev. B **63**, 144519 (2001).
24) T. C. Kobayashi, K. Hanazono, N. Tateiwa, K. Amaya, Y. Haga, R. Settai, and Y. Ōnuki, J. Phys.: Condens. Matter **14**, 10779 (2002).
25) A. Miyake, D. Aoki, and J. Flouquet, J. Phys. Soc. Jpn. **77**, 094709 (2008).
26) F. Hardy, D. Aoki, C. Meingast, P. Schweiss, P. Burger, H. Löhneysen, and J. Flouquet, Phys. Rev. B **83**, 195107 (2011).
27) Y. Noma, H. Kotegawa, T. Kubo, H. Tou, H. Harima, Y. Haga, E. Yamamoto, Y. Ōnuki, K. M. Itoh, E. E. Haller, A. Nakamura, Y. Homma, F. Honda, and D. Aoki, Physica B in press (available online).
28) N. Tateiwa, K. Hanazono, T. C. Kobayashi, K. Amaya, T. Inoue, K. Kindo, Y. Koike, N. Metoki, Y. Haga, R. Settai, and Y. Ōnuki, J. Phys. Soc. Jpn. **70**, 2876 (2001).
29) F. Hardy, C. Meingast, V. Taufour, J. Flouquet, H. v. Löhneysen, R. A. Fisher, N. E. Phillips, A. Huxley, and J. C. Lashley, Phys. Rev. B **80**, 174521 (2009).
30) R. Troć, Z. Gajek, and A. Pikul, Phys. Rev. B **86**, 224403 (2012).
31) A. Palacio Morales, A. Pourret, G. Knebel, G. Bastien, V. Taufour, D. Aoki, H. Yamagami, and J. Flouquet, Phys. Rev. B **93**, 155120 (2016).
32) T. Moriya and K. Ueda, Solid State Commun. **15**, 169 (1974).
33) J. Chepin and J. H. Ross, Jr., J. Phys.: Condens. Matter **3**, 8103 (1991).